
Turbulence and CFD models: Theory and applications

Roadmap to Lecture 9

- 1. Favre averaging**
- 2. RANS models corrections**
- 3. Wall functions for heat transfer**
- 4. Wall functions – Additional observations**
- 5. Surface roughness**
- 6. Non-linear eddy viscosity models**

Roadmap to Lecture 9

- 1. Favre averaging**
2. RANS models corrections
3. Wall functions for heat transfer
4. Wall functions – Additional observations
5. Surface roughness
6. Non-linear eddy viscosity models

Favre averaging

- When dealing with compressible flows (or variable density flows), besides the velocity and pressure fluctuations, we must also account for density and temperature fluctuations.
- If we use the Reynolds decomposition and time-averaging additional fluctuating correlations arise.
- To illustrate this, let us consider the conservation of mass equations for a compressible flow,

$$\frac{\partial \rho}{\partial t} + \nabla \cdot (\rho \mathbf{u}) = 0$$

- Now, let us use the Reynolds decomposition for the primitive variables (density and velocity),

$$\phi(\mathbf{x}, t) = \bar{\phi}(\mathbf{x}) + \phi'(\mathbf{x}, t) \quad \text{or} \quad \phi(\mathbf{x}, t) = \bar{\phi}(\mathbf{x}, t) + \phi'(\mathbf{x}, t)$$

Favre averaging

- Substituting the Reynolds decomposition into the continuity equation yields,

$$\frac{\partial(\bar{\rho} + \rho')}{\partial t} + \nabla \cdot (\bar{\rho}\mathbf{u} + \rho'\mathbf{u} + \bar{\rho}\mathbf{u}' + \rho'\mathbf{u}') = 0$$

- By time averaging the previous equation and using the Reynolds averaging rules, we arrive to the Reynolds-averaged continuity equation for compressible flows,

$$\frac{\partial(\bar{\rho})}{\partial t} + \nabla \cdot (\bar{\rho}\bar{\mathbf{u}} + \overline{\rho'\mathbf{u}'}) = 0$$

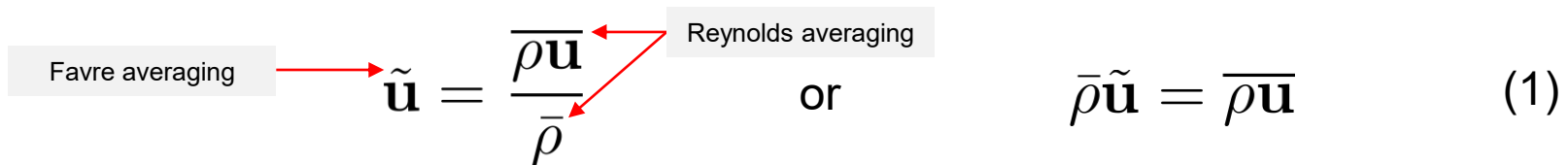
- To achieve closure, we need to somehow approximate the correlation between the fluctuating quantities ($\overline{\rho'\mathbf{u}'}$).
- The situation is more complicated for the momentum and energy equations, where triple correlations involving the density fluctuations appear.

Favre averaging

- To simplify the problem, we introduce the density-weighted averaging procedure suggested by Favre [1].
- That is, we introduce the mass-weighted average of the quantity ϕ , as follows,

$$\tilde{\phi} = \frac{1}{\bar{\rho}} \lim_{T \rightarrow \infty} \frac{1}{T} \int_t^{t+T} \rho(\mathbf{x}, t) \phi(\mathbf{x}, t) dt = \frac{\overline{\rho \phi}}{\bar{\rho}}$$

- For example, the mass-weighted average of the velocity field is given as follows,



$$\tilde{\mathbf{u}} = \frac{\overline{\rho \mathbf{u}}}{\bar{\rho}} \quad \text{or} \quad \bar{\rho} \tilde{\mathbf{u}} = \overline{\rho \mathbf{u}} \quad (1)$$

- In our notation, the overbar denotes Reynolds averaging and the tilde denotes Favre averaging.
- If we expand the RHS of equation 1 (that is, we substitute the Reynolds decomposition and use the Reynolds averaging rules), we obtain,

$$\bar{\rho} \tilde{\mathbf{u}} = \bar{\rho} \bar{\mathbf{u}} + \overline{\rho' \mathbf{u}'}$$

Favre averaging

- If we substitute the following relation,

$$\bar{\rho}\tilde{\mathbf{u}} = \bar{\rho}\bar{\mathbf{u}} + \overline{\rho'\mathbf{u}'}$$

- Into the Reynolds averaged compressible continuity equation,

$$\frac{\partial(\bar{\rho})}{\partial t} + \nabla \cdot (\bar{\rho}\bar{\mathbf{u}} + \overline{\rho'\mathbf{u}'}) = 0$$

- We obtain the following equation,

$$\frac{\partial(\bar{\rho})}{\partial t} + \nabla \cdot (\bar{\rho}\tilde{\mathbf{u}}) = 0$$

- This is the Favre averaged compressible continuity equation.
- Which looks very similar to the incompressible Reynolds averaged equations.
- As for the Reynolds averaged equations, we simply eliminated the correlation of the fluctuating quantities.
- We can proceed in a similar fashion for the momentum and energy equations.

Favre averaging

- Like the Reynolds decomposition, we can introduce a Favre decomposition of the variable ϕ , as follows,

$$\phi = \tilde{\phi} + \phi''$$

Notice that this fluctuating quantity also includes the effects of density fluctuations

- And to form a Favre average, we simply multiply by the density and do time average (in the same way as in Reynolds average),

$$\overline{\rho\phi} = \bar{\rho}\tilde{\phi} + \overline{\rho\phi''}$$

- And recall that the mass-weighted average of the field ϕ is given as follows,

$$\tilde{\phi} = \frac{\overline{\rho\phi}}{\bar{\rho}}$$

- It is important to mention that density and pressure are not mass-weighted averaged.
- For density and pressure, we use Reynolds averaging (that is, Reynolds decomposition).
- The rest of the field variables can be mass-weighted averaged, namely, u, v, w, T, h, H, e .

Favre averaging

- At this point, the rules of Favre averaging are summarized as follows,

$$\bar{\tilde{\phi}} = \tilde{\phi}$$

$$\overline{\rho \tilde{\phi}} = \bar{\rho} \tilde{\phi}$$

$$\overline{\rho \phi''} = 0$$

$$\overline{\phi''} = -\frac{\overline{\rho' \phi'}}{\bar{\rho}} \neq 0$$

$$\overline{\rho \phi \psi} = \bar{\rho} \tilde{\phi} \tilde{\psi} + \overline{\rho \phi'' \psi''}$$

$$\widetilde{\rho \phi} = \bar{\rho} \tilde{\phi}$$

- Plus the Reynolds averaging rules.
- Finally, if the density is constant, $\tilde{\phi} = \bar{\phi}$ and $\phi'' = \phi'$, and we recast the incompressible RANS equations.

Favre averaging

- The Favre-averaged governing equations can be written as follows (using index notation),

$$\frac{\partial \bar{\rho}}{\partial t} + \frac{\partial}{\partial x_i} (\bar{\rho} \tilde{u}_i) = 0$$

$$\frac{\partial \bar{\rho} \tilde{u}_i}{\partial t} + \frac{\partial \bar{\rho} \tilde{u}_j \tilde{u}_i}{\partial x_j} = -\frac{\partial P}{\partial x_i} + \frac{\partial}{\partial x_j} \left[\bar{\tau}_{ji} - \overline{\rho u_j'' u_i''} \right]$$

$$\frac{\partial}{\partial t} \left[\bar{\rho} \left(\tilde{e} + \frac{\tilde{u}_i \tilde{u}_i}{2} \right) + \frac{\overline{\rho u_i'' u_i''}}{2} \right] + \frac{\partial}{\partial x_j} \left[\bar{\rho} \tilde{u}_j \left(\tilde{h} + \frac{\tilde{u}_i \tilde{u}_i}{2} \right) + \tilde{u}_j \frac{\overline{\rho u_i'' u_i''}}{2} \right] =$$

$$\frac{\partial}{\partial x_j} \left[-q_{Lj} - \overline{\rho u_j'' h''} + \overline{\tau_{ji} u_j''} - \overline{\rho u_j'' \frac{1}{2} u_i'' u_i''} \right] + \frac{\partial}{\partial x_j} \left[\tilde{u}_i \left(\bar{\tau}_{ij} - \overline{\rho u_i'' u_j''} \right) \right]$$

$$P = \bar{\rho} R \tilde{T}$$

- These are the exact FANS equations (Favre-averaged Navier-Stokes).
- As for the RANS equations, we need to add approximations to derive the solvable equations.

Favre averaging

- Let us review the most commonly used approximations for compressible flows.
 - Reynolds-Stress tensor (or Favre-Stress tensor),

$$\bar{\rho}\tau_{ij}^F = \overline{-\rho u_i'' u_j''} = \mu_T \left(\frac{\partial \tilde{u}_i}{\partial x_j} + \frac{\partial \tilde{u}_j}{\partial x_i} - \frac{2}{3} \frac{\partial \tilde{u}_k}{\partial x_k} \delta_{ij} \right) - \frac{2}{3} \bar{\rho} k \delta_{ij}$$

- Turbulent heat-flux vector,

$$q_{Tj} = \overline{\rho u_j'' h''} = -\frac{\mu_T c_p}{Pr_T} \frac{\partial \tilde{T}}{\partial x_j} = -\frac{\mu_T}{Pr_T} \frac{\partial \tilde{h}}{\partial x_j}$$

- Molecular diffusion and turbulent transport,

$$\overline{\tau_{ji} u_i''} - \overline{\rho u_j'' \frac{1}{2} u_i'' u_i''} = \left(\mu + \frac{\mu_T}{\sigma_k} \right) \frac{\partial k}{\partial x_j}$$

Favre averaging

- It is important to mention that for compressible flows, the non-zero divergence of the Favre averaged velocity modifies the mean strain rate term in the RHS of the Reynolds-Stress tensor.
- Therefore, the Reynolds-Stress tensor is manipulated in such a way to guarantee that its trace is equal to $-2k$.
- This implies that the second eddy viscosity is equal to,

$$\frac{2}{3}\mu_T$$

- The turbulent kinetic energy can be computed as follows,

$$\bar{\rho}k = \frac{1}{2}\overline{\rho u_i'' u_i''}$$

- The viscous stress tensor τ_{ij} and the molecular heat flux q_L (or laminar) are computed as follows,

$$\tau_{ij} = \mu \left(\frac{\partial \tilde{u}_i}{\partial x_j} + \frac{\partial \tilde{u}_j}{\partial x_i} \right) - \frac{2}{3}\mu \frac{\partial \tilde{u}_k}{\partial x_k} \delta_{ij} \qquad q_L = -\kappa \frac{\partial \tilde{T}}{\partial x_j}$$

Favre averaging

- As it can be seen, the Favre averaging is very similar to the Reynolds averaging.
- To derive the solvable equations, we must approximate all the terms that involve correlations of fluctuating quantities.
- Similar to the incompressible equations, we can derive the exact transport equations for the turbulent kinetic energy and Reynolds stresses.
- Favre averaging is used for compressible flows, mixture of gases, species concentration, and combustion.
- Favre averaging eliminates density fluctuations from the averaged equations.
- However, it does not remove the effect the density fluctuations have on the turbulence.
- Favre averaging is a mathematical simplification, not a physical one.
- Remember, when using Favre averaging, the density and pressure are not mass-weighted averaged.

Roadmap to Lecture 9

- ~~1. Favre averaging~~
- 2. RANS models corrections**
3. Wall functions for heat transfer
4. Wall functions – Additional observations
5. Surface roughness
6. Non-linear eddy viscosity models

RANS models corrections

- The Boussinesq approximation (or EVM) is a brutal simplification of reality, and this can be a major source of predictive defects.
- And this is regardless of the closure approximations used (turbulence models), which are, in themselves, the cause of additional errors.
- The Boussinesq approximation lies in the belief that the Reynolds Stress tensor behaves in a similar fashion as the Newtonian viscous stress tensor.
- The EVM models assume a linear behavior of the Reynolds stress tensor.
- The main deficiencies of the EVM models are:
 - The assumption of isotropy in shear flows (which is not strictly true),

$$\overline{u'^2} = \overline{v'^2} = \overline{w'^2} = \frac{2}{3}k$$

- The possibility of predicting negative normal shear stresses.

RANS models corrections

- Let us summarize a few applications where the Boussinesq approximation is not very accurate,
 - Poor performance in flows with large extra strains, *e.g.*, curved surfaces, strong vorticity, swirling flows.
 - Rotating flows, *e.g.*, turbomachinery, wind turbines.
 - Impinging flows.
 - Highly anisotropic flows and flows with secondary motions, *e.g.*, fully developed flows in non-circular ducts.
 - Non-local equilibrium and flow separation, *e.g.*, airfoil in stall, dynamic stall.
 - Complex three-dimensional flows.
 - Residual turbulent viscosity near the walls.
- Many EVM models has been developed and improved along the years so they address the shortcomings of the Boussinesq approximation.

RANS models corrections

- In spite of the theoretical weakness of the Boussinesq approximation, it does produce reasonable results for a large number of flows.
- EVM models are the cornerstone of turbulence modeling in industrial applications.
- EVM is an area of active research and new ideas and palliatives to the known deficiencies continues to emerge.
- Many of the corrections take the form of:
 - Additional source terms.
 - Extra terms in the transport equations.
 - Corrective factors (damping, blending, limiting) in some of the terms of the transport equations.
- Let us briefly overview a few of the remedies to some of the problems found with EVM.

RANS models corrections

- Let us recall the Boussinesq approximation.
- Remember, this approximation is the core of all eddy viscosity models (EVM).

$$\tau^R = -\rho \overline{(\mathbf{u}'\mathbf{u}')} = 2\mu_T \overline{\mathbf{D}}^R - \frac{2}{3}\rho k \mathbf{I} = \mu_T \left[\nabla \bar{\mathbf{u}} + (\nabla \bar{\mathbf{u}})^T \right] - \frac{2}{3}\rho k \mathbf{I}$$

Reynolds averaged strain-rate tensor

Identity matrix (or Kronecker delta).

$$\overline{\mathbf{D}}^R = \frac{1}{2} (\nabla \bar{\mathbf{u}} + \nabla \bar{\mathbf{u}}^T) \quad k = \frac{1}{2} \overline{\mathbf{u}' \cdot \mathbf{u}'} = \frac{1}{2} \left(\overline{u'^2} + \overline{v'^2} + \overline{w'^2} \right)$$

$$\mathbf{I} = \begin{bmatrix} 1 & 0 & 0 \\ 0 & 1 & 0 \\ 0 & 0 & 1 \end{bmatrix}$$

Which is equivalent to the Kronecker delta

$$\delta_{ij} = \begin{cases} 1, & \text{if } i = j, \\ 0, & \text{if } i \neq j. \end{cases}$$

RANS models corrections

Production limiters

- A disadvantage of two-equation turbulence models is the excessive generation of the turbulent kinetic energy in the vicinity of stagnation points.
- Many corrections have been proposed to avoid this problem.
- Let us discuss a production limiter approach originally proposed by Menter [1].
- In order to avoid the buildup of turbulent kinetic energy in the stagnation regions, the production term in the turbulence equations can be limited as follows,

$$P_k = \min (P_k, C_{lim} \rho \epsilon)$$

- Where the coefficient C_{lim} has a default value of 10.
- This limiter does not affect the shear layer performance of the model, but it avoids the stagnation point buildup in aerodynamic simulations.
- Another formulation is based on the work of Kato and Launder [2].

[1] F. R. Menter. Two-Equation Eddy-Viscosity Turbulence Models for Engineering Applications. AIAA Journal. 32(8). 1598–1605. August 1994.
[2] M. Kato and B. E. Launder. The modelling of turbulent flow around stationary and vibrating square cylinders. Ninth Symposium on Turbulent Shear Flows. Kyoto, Japan. August 16-18, 1993.

RANS models corrections

Curvature correction

- One drawback of the eddy-viscosity models is that these models are insensitive to streamline curvature and system rotation, which play a significant role in many turbulent flows of practical interest.
- Spalart and Shur [1], Shur et al. [2], and Smirnov and Menter [3], have proposed a modification to the production term in order to sensitize EVM models to the effects of streamline curvature and system rotation,

$$P_k \rightarrow P_k f_r$$

$$f_r = \max \left[0, 1 + C_{curv} \left(\tilde{f}_r - 1 \right) \right] \quad \tilde{f}_r = \max \left[\min (f_{rotation}, 1.25), 0 \right]$$

$$f_{rotation} = (1 + C_{r1}) \frac{2r^*}{1 + r^*} \left[1 - C_{r3} \tan^{-1} (C_{r2} \tilde{r}) \right] - C_{r1} \quad C_{curv} \quad \text{Coefficient to allow influence the strength of the curvature correction}$$

- The rest of the closure coefficient and relationships can be found in reference [1].

[1] P. R. Spalart, M. L. Shur. On the Sensitization of Turbulence Models to Rotation and Curvature. Aerospace Sci. Tech. 1(5). 297–302. 1997.

[2] M. L. Shur, M. K. Strelets, A. K. Travin, P. R. Spalart. Turbulence Modeling in Rotating and Curved Channels: Assessing the Spalart-Shur Correction. AIAA Journal. 38(5). 2000.

[3] P. E. Smirnov, F. R. Menter. Sensitization of the SST Turbulence Model to Rotation and Curvature by Applying the Spalart-Shur Correction Term. ASME Paper GT 2008-50480. 2008.

RANS models corrections

Prediction of excessive heat transfer

- In separated or impinging flows, the near-wall length-scale can become too large, resulting in excessively high levels of near-wall turbulence.
- To remedy this behavior, Yap [1] introduced an extra source term into the dissipation rate equation.
- The modification, which is used on the ϵ transport equation is given as follows,

$$S_{\epsilon} = 0.83 \frac{\epsilon^2}{k} \max \left[\left(\frac{l}{\epsilon l_e} - 1 \right) \left(\frac{l}{\epsilon l_e} \right)^2, 0 \right] \quad \text{where} \quad l = \frac{k^{1.5}}{\epsilon} \quad l_e = C_{\mu}^{-0.75} \kappa y$$

- This correction is useful to prevent excessive heat transfer at re-attachment and stagnation points.
- To eliminate the dependence of the above source term on the wall distance, a differential form of the length-scale correction was proposed in reference [2].

[1] C. Yap. Turbulent heat and momentum transfer in recirculating and impinging flows . Ph.D. Thesis Manchester University. 1987.

[2] H. Iacovides, M. Raisee. Recent progress in the computation of flow and heat transfer in internal cooling passages of gas turbine blades. Int. J. Heat Fluid Flow 20:320–328. 1999.

RANS models corrections

Realizability

- The term realizability is related to physically tenable Reynolds stress predictions.
- In easier terms, a realizable stated is one in which none of the normal stresses becomes negative, *i.e.*,

$$\overline{u'^2}, \overline{v'^2}, \overline{w'^2} \geq 0$$

- In addition, realizability also satisfy the following condition,

$$\frac{\overline{uv}}{\sqrt{\overline{u'^2}} \sqrt{\overline{v'^2}}}, \frac{\overline{uw}}{\sqrt{\overline{u'^2}} \sqrt{\overline{w'^2}}}, \frac{\overline{vw}}{\sqrt{\overline{v'^2}} \sqrt{\overline{w'^2}}} < 1$$

- The previous relations are referred to as the Schwartz inequality.
- These inequalities can be enforced in EVM models.
- The most known model that satisfy this inequality is the Realizable $k - \epsilon$.

RANS models corrections

Damping functions near the walls

- Near the walls, in the viscous sublayer, the turbulent viscosity should exponentially damp to zero.
- Some EVM models might have prediction capability issues since they predict non-zero values (or large values) of turbulent viscosity near the walls.
- To correct this behavior, many EVM use damping functions near the walls.
- For the example, the Van Driest damping function commonly used in mixing length models, reads as follows,

$$l = \kappa y \left[1 - e^{-y^+/A^+} \right]$$

l is used as the length scale to compute the turbulent viscosity

$$A^+ = 26$$

This coefficient depends on the pressure gradient

- Another damping function used in the low-RE $k - \epsilon$ turbulence model by Jones and Launder [1], is written as follows,

$$\nu_t = C_\mu f_\mu \frac{k^2}{\epsilon}$$

$$f_\mu = e^{-2.5/(1+Re_T/50)}$$

$$Re_T = \frac{k^2}{\nu \epsilon}$$

Roadmap to Lecture 9

- ~~1. Favre averaging~~
- ~~2. RANS models corrections~~
- 3. Wall functions for heat transfer**
- ~~4. Wall functions – Additional observations~~
- ~~5. Surface roughness~~
- ~~6. Non-linear eddy viscosity models~~

Wall functions for heat transfer

- As for the momentum (or viscous) wall functions, there is also a treatment for the thermal wall functions.
- Depending on the value of y^* , the value of the non-dimensional temperature T^* (equivalent to the concept of u^*), can be computed as follows,

$$T^* = \begin{cases} Pr y^* & y^* < 5 \\ Pr_t \left[\frac{1}{\kappa} \ln(Ey^*) + P \right] & y^* > 30 \end{cases}$$

Thermal viscous sublayer where conduction is important

Molecular (or laminar) Prandtl number Pr

Turbulent Prandtl number Pr_t

Logarithmic law for the turbulent region where effects of turbulence dominate conduction

- The nondimensional temperature relation (log-law region),

$$T^* = Pr_t \left[\frac{1}{\kappa} \ln(Ey^*) + P \right]$$

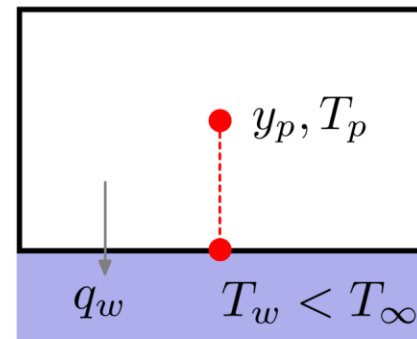
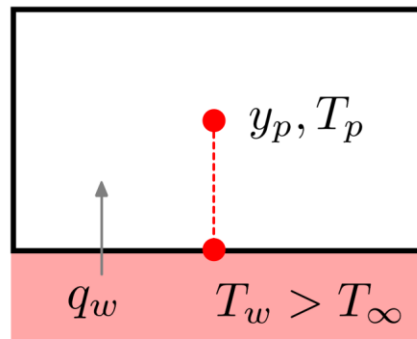
- It is used to relate the temperature at the cell center T_p to the heat flux at the wall q_w .
- This is similar to what we did with the viscous wall function, where we related U_p to τ_w .

Wall functions for heat transfer

- When using thermal wall functions, we are interested in computing the thermal diffusivity used to approximate the wall heat transfer q_w ,

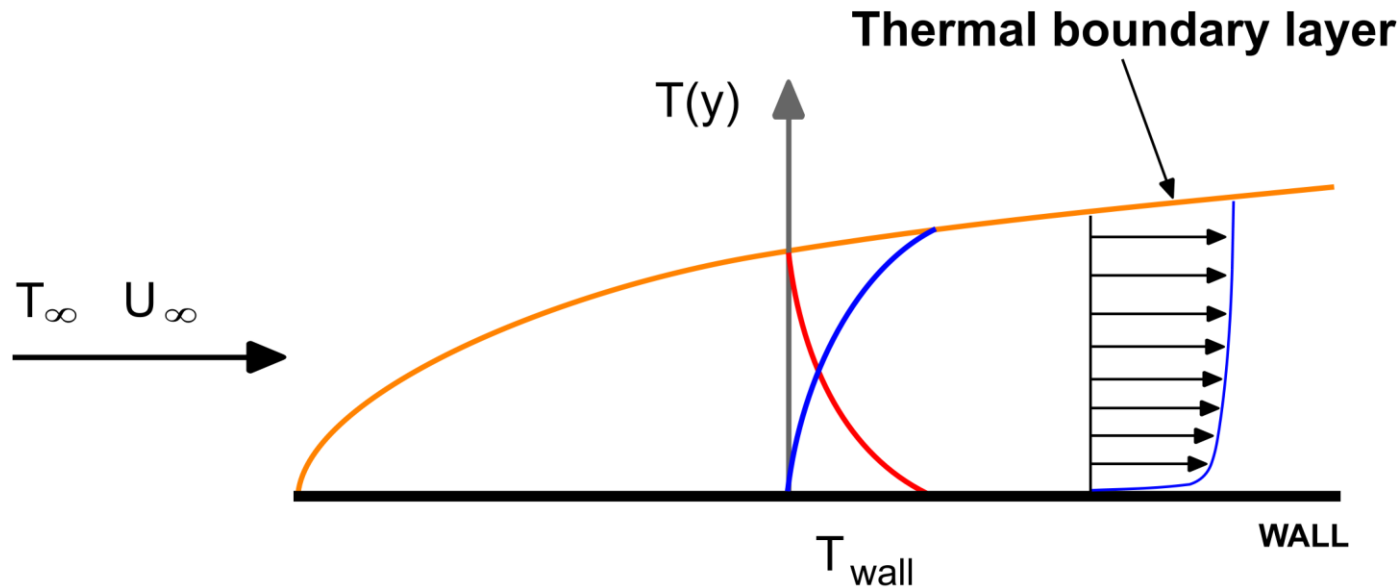
$$q_w = \underbrace{k}_{\text{Thermal conductivity}} \frac{\partial T}{\partial y} = \rho \underbrace{c_p \alpha}_{\text{Thermal diffusivity}} \frac{\partial T}{\partial y} = \underbrace{\rho c_p \alpha}_{\text{Specific heat}} \frac{T_w - T_p}{y_p - y_w}$$

- We need to relate the temperature at the cell center T_p to the heat flux at the wall q_w .



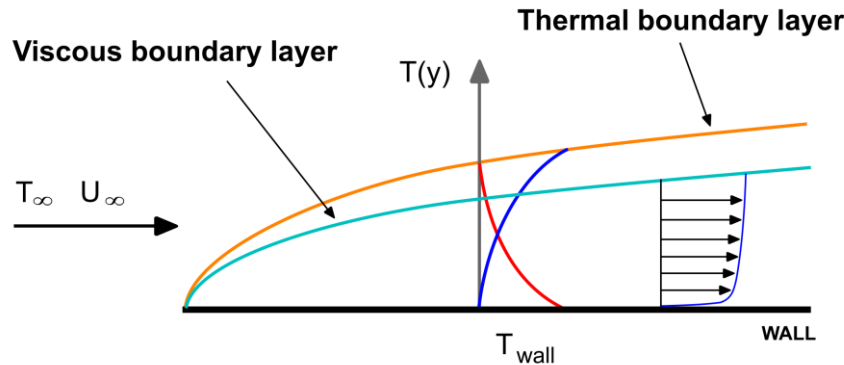
Wall functions for heat transfer

- Recall that in the momentum boundary layer, the velocity at the walls is zero.
- In the thermal boundary layer, the temperature at the wall can be higher or lower than the freestream temperature.
- Therefore, we can have very different temperature profiles growing from the walls.
- The temperature at the walls also has an influence of the wall shear stresses.

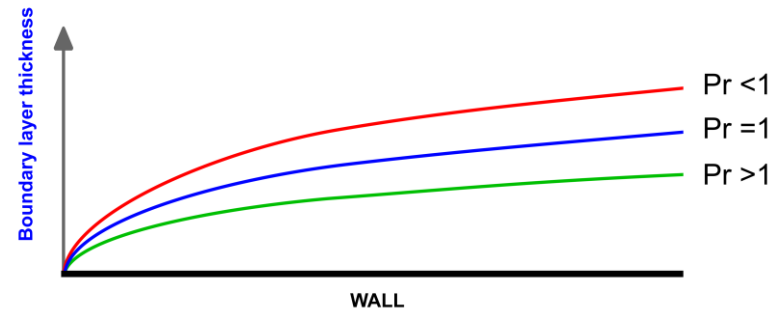


Wall functions for heat transfer

Momentum and thermal boundary layer



Thermal boundary layer vs. Viscous boundary layer
Forced convection

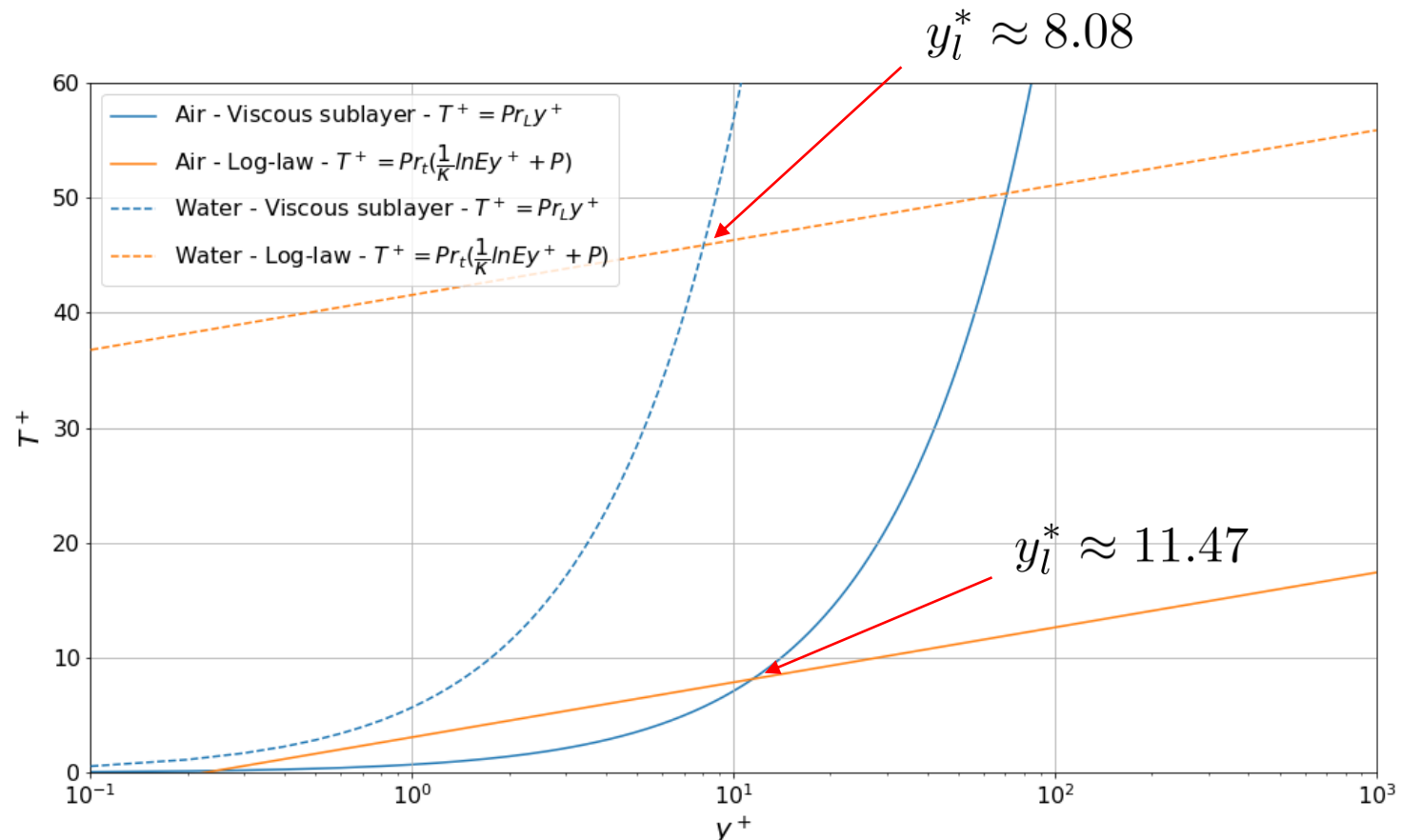


Thermal boundary layer in function of Prandtl number (Pr)

- Just as there is a viscous boundary layer in the velocity distribution (or momentum), there is also a thermal boundary layer.
- Thermal boundary layer thickness is different from the thickness of the viscous sublayer (momentum) and is fluid dependent.
- The thickness of the thermal sublayer for a high Prandtl number fluid (e.g. water) is much less than the momentum sublayer thickness.
- For fluids of low Prandtl numbers (e.g., air), it is much larger than the momentum sublayer thickness.
- For Prandtl number equal 1, the thermal boundary layer is equal to the momentum boundary layer.

Wall functions for heat transfer

- The normalized temperature plot (T^+ vs. y^+), depends on the Prandtl number.
- Different values of Prandtl number will result in different plots, with different intersection points between the viscous sublayer and the log-law region.
- The intersection point of the viscous sublayer and the log-law region is known as the non-dimensional thermal sublayer thickness or y_l^* .



Wall functions for heat transfer

- The thermal diffusivity coefficient α is computed as follows,

$$\alpha_w = \begin{cases} \alpha & y^* < y_l^* \\ \frac{u_\tau y_p}{Pr_t \left[\frac{1}{\kappa} \ln(Ey^*) + P \right]} & y^* > y_l^* \end{cases}$$

- Remember, the value of y_l^* depends on the Prandtl number.
- At this point, the heat flux q_w at the wall can be computed as follows,

$$q_w = \rho c_p \alpha_w \frac{T_w - T_p}{y_p - y_w}$$

- The turbulent Prandtl number Pr_t is usually equal to 0.85, but it highly depends on the flow properties and the flow physics.

Wall functions for heat transfer

- Let us revisit the nondimensional temperature function T^* ,

$$T^* = Pr_t \left[\frac{1}{\kappa} \ln(Ey^*) + P \right] \quad y^* > 30$$

- The term P appearing in this relation, has a strong dependence on the Prandtl number (molecular and turbulent).
- One way to approximate this term is by using Jayatilleke function [1],

$$P = 9.24 \left[\left(\frac{Pr}{Pr_t} \right)^{3/4} - 1 \right] \left[1 + 0.28e^{-0.007Pr/Pr_t} \right]$$

- Kader [2] and Patankar and Spalding [3] also proposed alternative formulations for computing P .

[1] C. Jayatilleke. The influence of Prandtl number and surface roughness on the resistance of the laminar sublayer to momentum and heat transfer. Prog. Heat Mass Transfer, 1, 193-329. 1969.

[2] B. Kader. Temperature and concentration profiles in fully turbulent boundary layers. Int. J. Heat Mass Transfer. 24(9). 1981.

[3] S. Patankar and D. Spalding. A calculation procedure for heat, mass and momentum transfer in three dimensional parabolic flows. Int. J. Heat Mass Transfer, 15(10). 1972.

Wall functions for heat transfer

- Let us summarize the steps needed to compute the wall heat flux q_w using wall functions,
 - Compute y^* .
 - Compute the Prandtl number,

$$Pr = \frac{\nu}{\alpha}$$

- Compute the intersection point y_l^* .
- Compute the thermal diffusivity at the wall.

$$\alpha_w = \begin{cases} \alpha & y^* < y_l^* \\ \frac{u_\tau y_p}{Pr_t \left[\frac{1}{\kappa} \ln(Ey^*) + P \right]} & y^* > y_l^* \end{cases}$$

- Compute the heat flux at the wall.

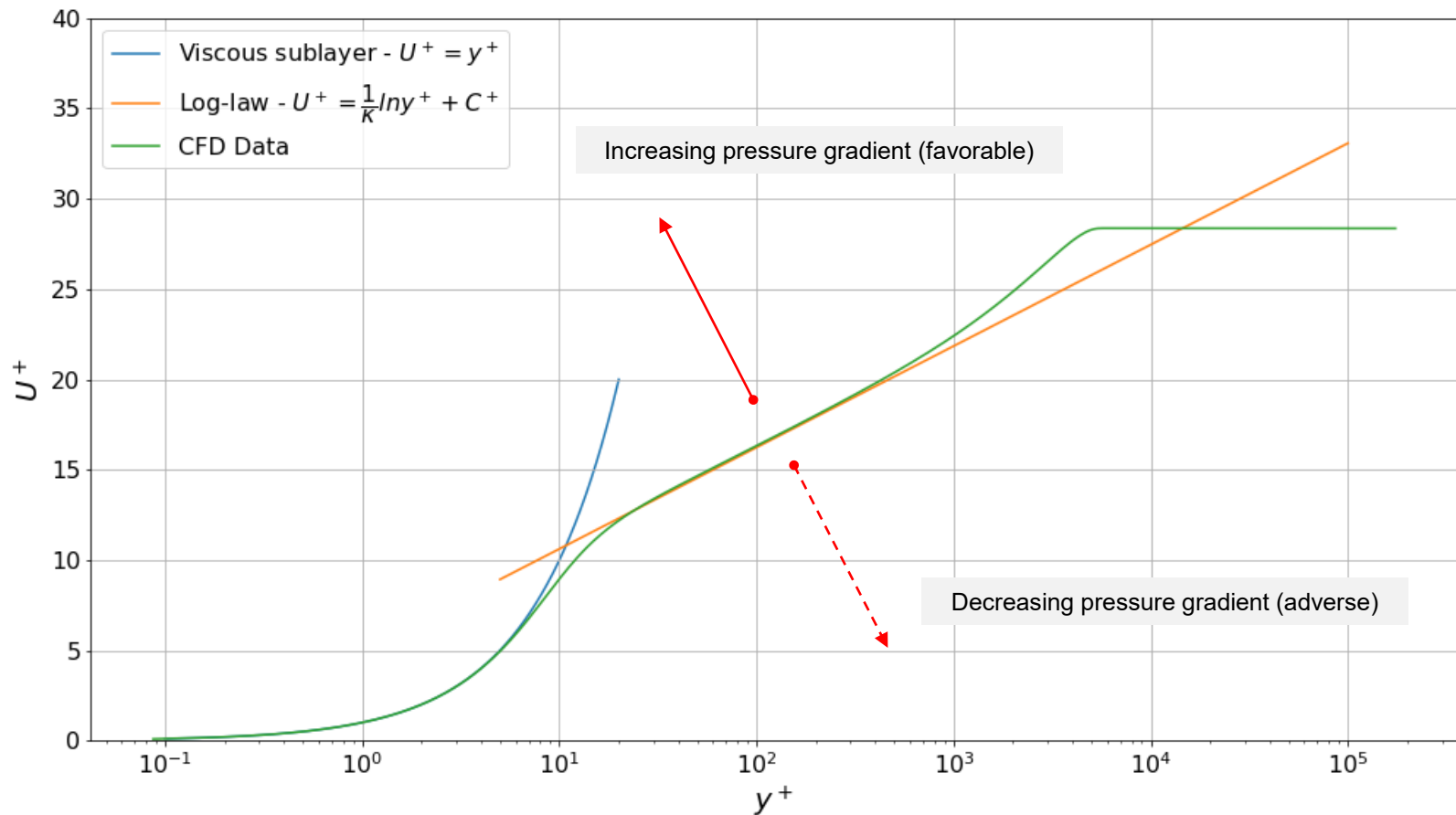
$$q_w = \rho c_p \alpha_w \frac{T_w - T_p}{y_p - y_w}$$

Roadmap to Lecture 9

- ~~1. Favre averaging~~
- ~~2. RANS models corrections~~
- ~~3. Wall functions for heat transfer~~
- 4. Wall functions – Additional observations**
- ~~5. Surface roughness~~
- ~~6. Non-linear eddy viscosity models~~

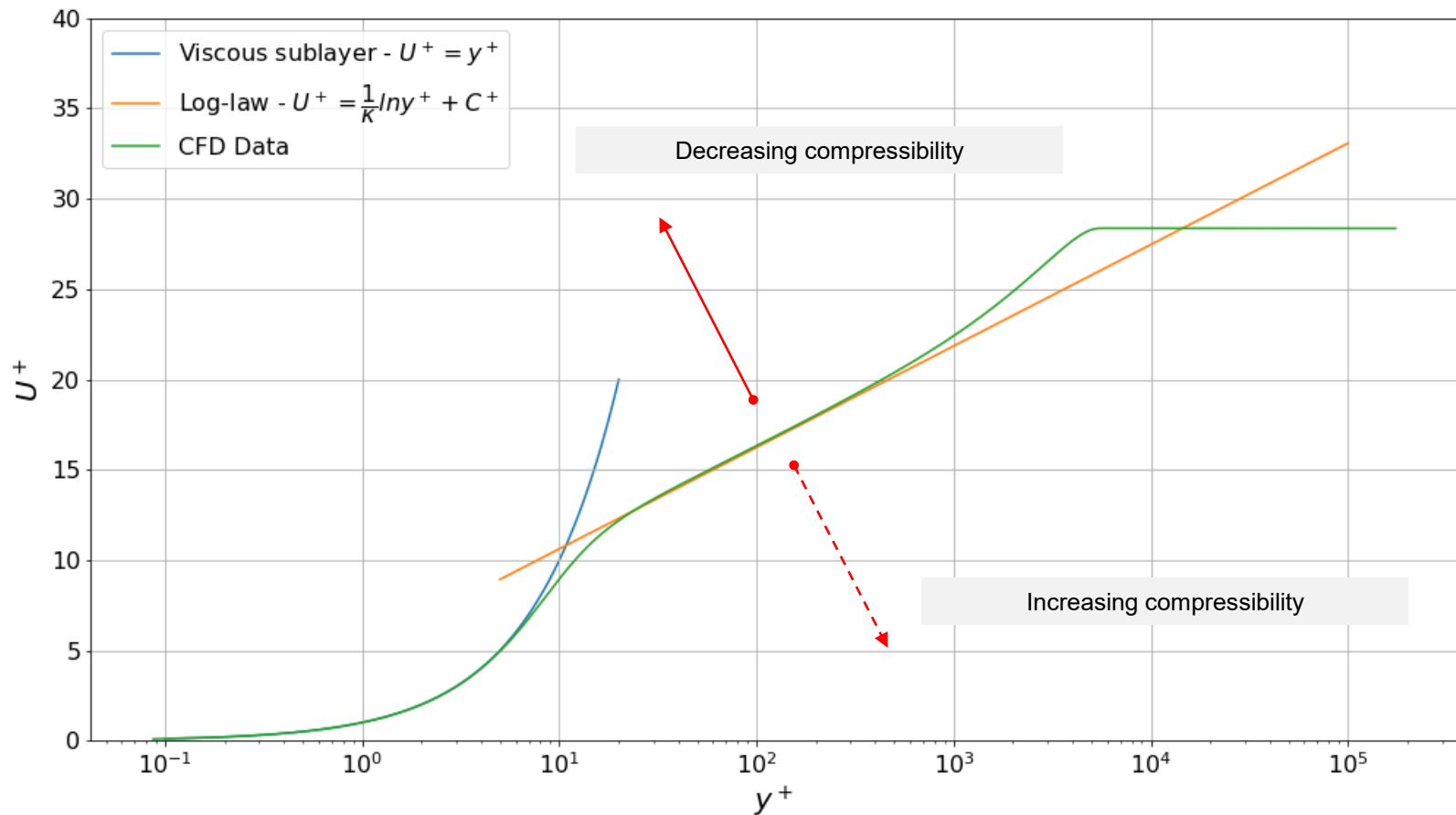
Wall functions – Additional observations

- Effect of adverse pressure gradient on the law of the wall.



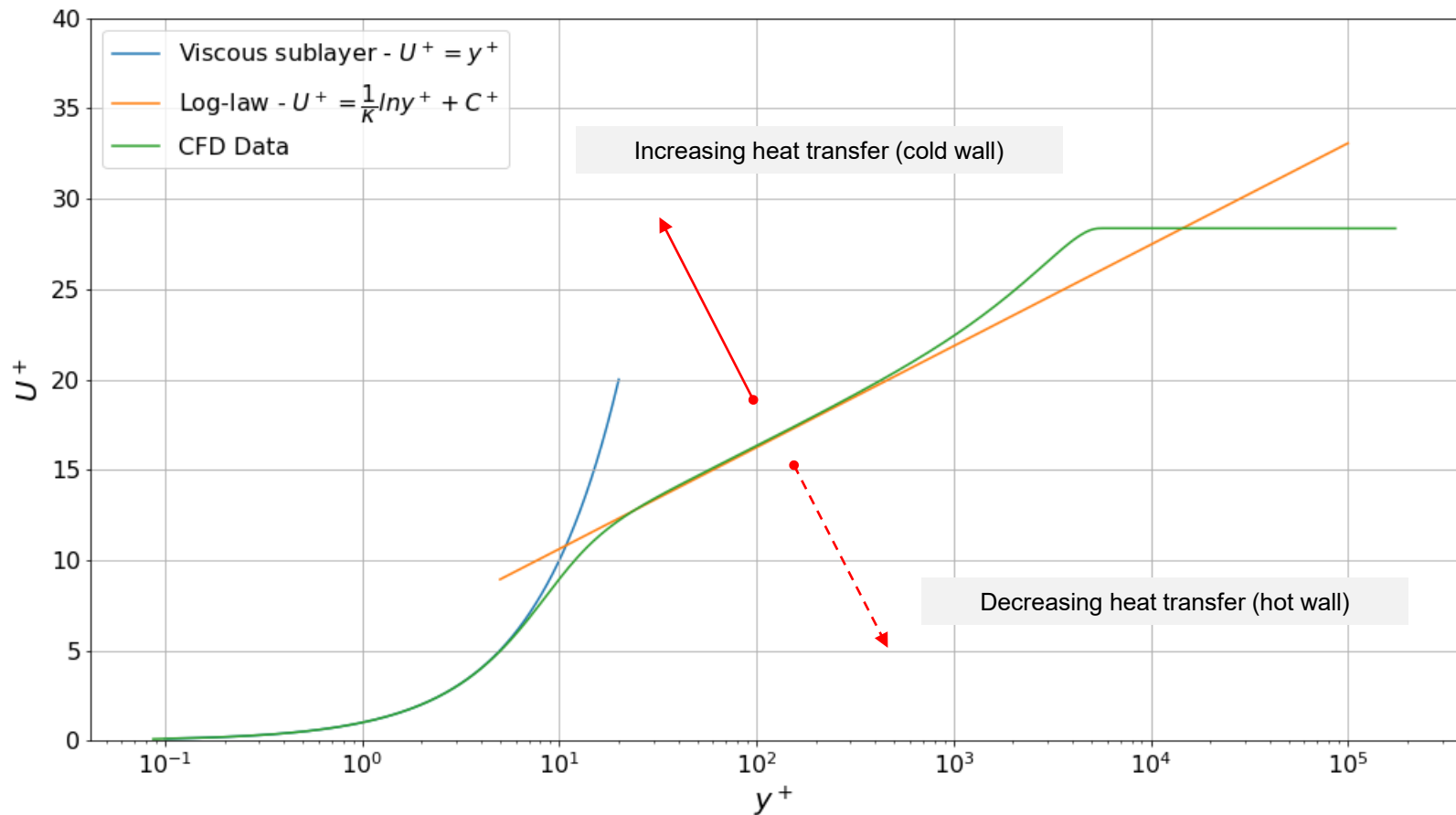
Wall functions – Additional observations

- Effect of compressibility on the law of the wall.



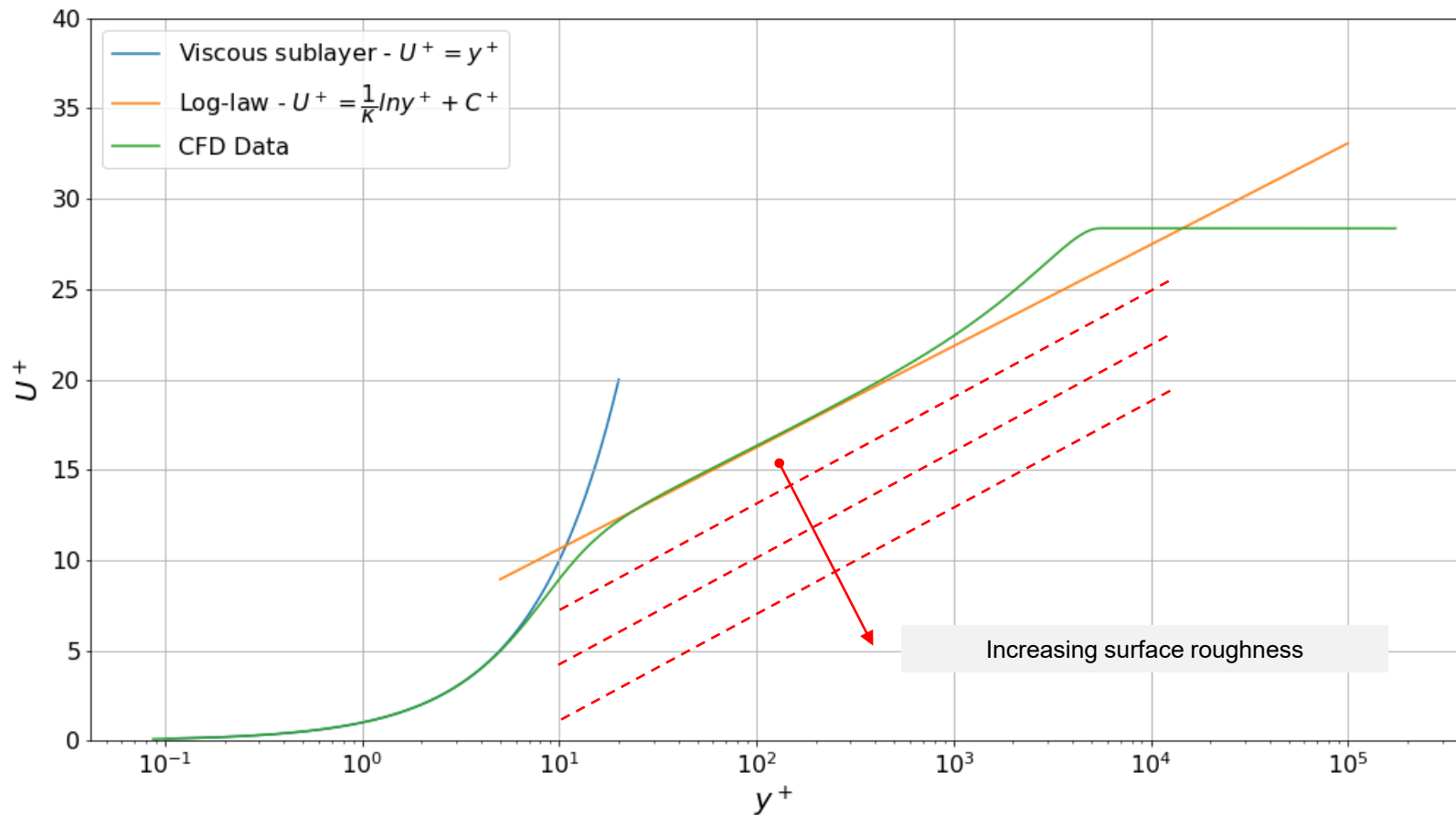
Wall functions – Additional observations

- Effect of heat transfer on the law of the wall.



Wall functions – Additional observations

- Effect of surface roughness on the law of the wall.



Wall functions – Additional observations

- When dealing with high speed flows and heat transfer, the coefficients appearing in the law of the wall relations and closure relations, have a strong dependence on the Mach number and the heat transfer rate.
- No need to mention that the physical properties also depend on the Mach number and heat transfer rate.

$$u^* = \begin{cases} y^* & y^* < 11.225 \\ \frac{1}{\kappa} \ln(y^*) + C & y^* > 11.225 \end{cases}$$

$$T^* = \begin{cases} Pr y^* & y^* < 5 \\ Pr_t \left[\frac{1}{\kappa} \ln(Ey^*) + P \right] & y^* > 30 \end{cases}$$

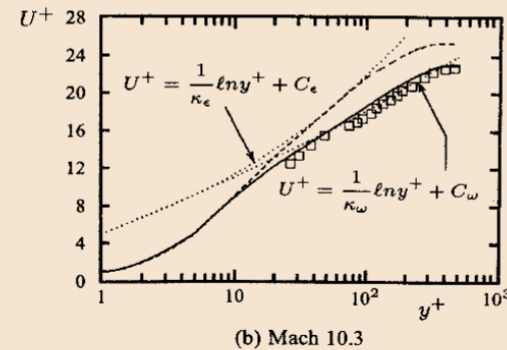
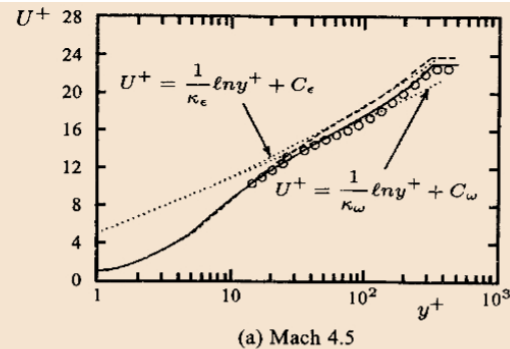


Figure 5.3: Computed and measured velocity profiles for compressible flat-plate boundary layers: — Wilcox (2006) $k-\omega$; - - Chien $k-\epsilon$; \circ Coles; \square Watson.

Wall functions – Additional observations

- In the case of pressure gradients and flow separation (non-equilibrium conditions), the law of the wall can be sensitized to pressure gradients effects [1].

$$\frac{\tilde{U} C_\mu^{1/4} k^{1/2}}{\tau_w / \rho} = \frac{1}{\kappa} \ln \left(E \frac{\rho C_\mu^{1/4} k^{1/2} y}{\mu} \right)$$

- Where,

$$\tilde{U} = U - \frac{1}{2} \frac{dp}{dx} \left[\frac{y_v}{\rho \kappa k^{1/2}} \ln \left(\frac{y}{y_v} \right) + \frac{y - y_v}{\rho \kappa k^{1/2}} + \frac{y_v^2}{\mu} \right]$$

$$y_v = \frac{\mu y_v^*}{\rho C_\mu^{1/4} k_p^{1/2}} \qquad y_v^* = 11.225$$

- This correction is recommended for use in complex flows involving separation, reattachment, and impingement where the mean flow and turbulence are subjected to pressure gradients and rapid changes.
- In such flows, improvements can be obtained, particularly in the prediction of wall shear (skin-friction coefficient) and heat transfer (Nusselt or Stanton number).

Wall functions – Additional observations

- The non-dimensional temperature T^* , can be further improved by adding the viscous heating contribution [1],

$$T^* = T_c^* + \frac{D}{q}$$

- Where,

$$T_c^* = \begin{cases} Pr y^* & y^* < y_l^* \\ Pr_T \left[\frac{1}{\kappa} \ln(Ey^*) + P \right] & y^* > y_l^* \end{cases}$$

$$D = \begin{cases} \rho u^* \frac{1}{2} Pr U_p^2 & y^* < y_l^* \\ \rho u^* \frac{1}{2} [Pr_t U_p^2 + (Pr - Pr_t) U_c^2] & y^* > y_l^* \end{cases}$$

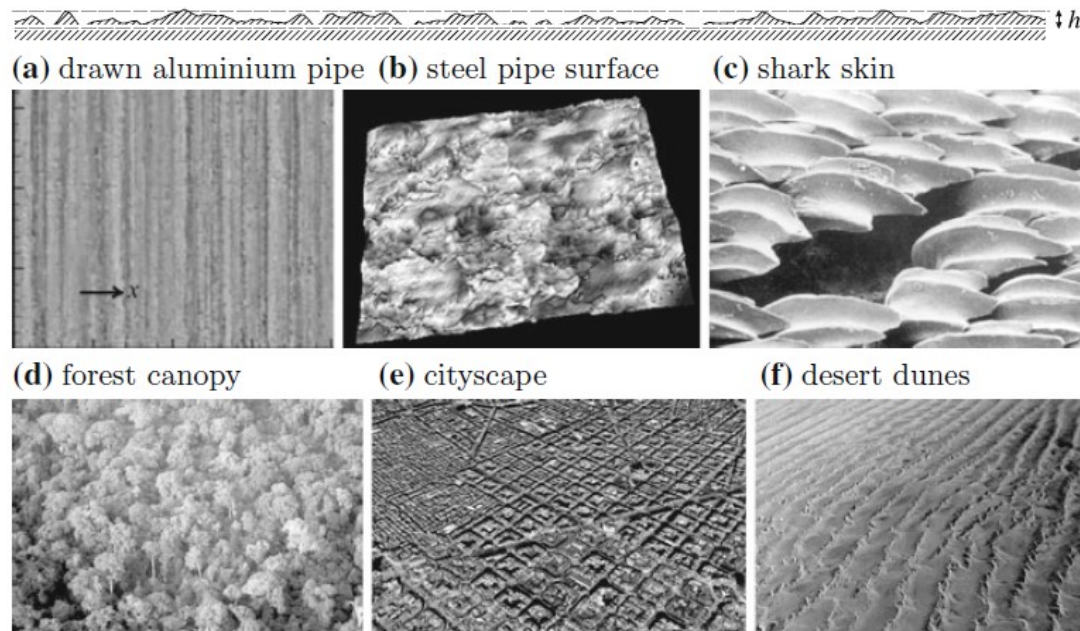
- Where U_c is the mean velocity at the intersection point y_l^* .
- This correction is recommended for highly compressible flows, where heating by viscous dissipation can have a strong influence in the temperature distribution in the near-wall region.

Roadmap to Lecture 9

- ~~1. Favre averaging~~
- ~~2. RANS models corrections~~
- ~~3. Wall functions for heat transfer~~
- ~~4. Wall functions – Additional observations~~
- 5. Surface roughness**
- ~~6. Non-linear eddy viscosity models~~

Surface roughness

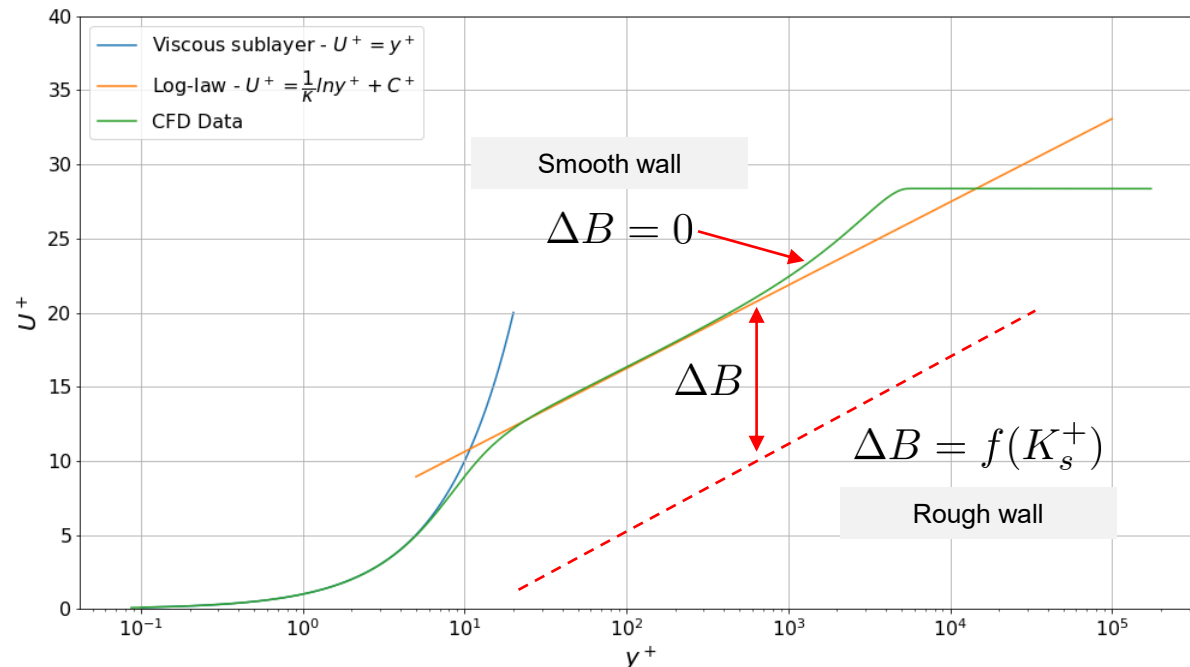
- So far, we have only considered smooth walls.
- In reality, every wall and material is characterized by small irregularities, which we refer to as roughness.
- The roughness have a characteristic height h , as shown in the figure below.
- Wall roughness increases the wall shear stress and heat transfer rate.



Examples of wall roughness. **(a)** Surface of an aluminum pipe: $h_{\text{rms}} \approx 0.16 \mu\text{m}$. **(b)** Scanned surface ($1.4 \times 1.1 \text{ mm}^2$) of a non-rusted commercial steel pipe: $h_{\text{rms}} \approx 5 \mu\text{m}$. **(c)** Scales of the great white shark: $h_{\text{rms}} \approx 0.1 \text{ mm}$. **(d)** Aerial views of tropical forest in Gabon ($h \approx 0.1\text{-}10 \text{ m}$). **(e)** Barcelona landscape ($h \approx 10\text{-}100 \text{ m}$). **(f)** The Namib desert ($h \approx 10\text{-}500 \text{ m}$). Adapted from reference [1].

Surface roughness

- In CFD, the roughness must be modeled.
- In theory, it can be resolved with very fine meshes but the computational requirements are too high.
- Wall roughness increases the wall shear stress and heat transfer rate.
- It also breaks up the viscous sublayer.
- By looking at the nondimensional velocity plot, the wall roughness shifts the nondimensional velocity downwards by a factor of ΔB .



Surface roughness

- There are many ways to add roughness to the solution.
- Let us study maybe the most common wall function for roughness.
- This implementation is based on the standard wall functions.

STEP 1.

$$U^+ = \frac{1}{\kappa} \ln(Ey^+) - \Delta B$$

← Roughness correction coefficient

STEP 2.

$$U^+ = \frac{1}{\kappa} \ln(Ey^+) - \ln(e^{\Delta B})$$

STEP 3.

$$U^+ = \frac{1}{\kappa} \ln\left(\frac{Ey^+}{e^{\Delta B}}\right)$$

- Where we used the following logarithm rules to derive the previous relations,

$$\ln(e^x) = x \qquad \ln(x) - \ln(y) = \ln\left(\frac{x}{y}\right)$$

Surface roughness

- If we introduce the following relation,

$$E' = \frac{E}{e^{\Delta B}}$$

- Into the relation corrected for wall roughness,

$$U^+ = \frac{1}{\kappa} \ln \left(\frac{E y^+}{e^{\Delta B}} \right)$$

- We obtain the following equation,

$$U^+ = \frac{1}{\kappa} \ln (E' y^+)$$

- Which is identical to the standard wall function formulation (except for the variable E').
- We now have a way to work with smooth and rough walls using the same log-law relation.

Surface roughness

- Let us now address the roughness correction factor ΔB .
- This factor can be computed as follows [1, 2],

$$\Delta B = 0 \quad K_s^+ < 2.25$$

Hydraulically smooth

$$\Delta B = \frac{1}{\kappa} \left(\frac{K_s^+ - 2.25}{87.75} + C_s K_s^+ \right) \times \dots$$
$$\dots \times \sin [0.4258 (\ln K_s^+ - 0.811)] \quad 2.25 < K_s^+ < 90$$

Transitional

$$\Delta B = \frac{1}{\kappa} \ln (1 + C_s K_s^+) \quad K_s^+ > 90$$

Fully rough

- Notice that ΔB is a function of the nondimensional roughness height K_s^+ and the roughness constant C_s .

[1] T. Cebeci, P. Bradshaw. Momentum Transfer in Boundary Layers. Hemisphere Publishing Corporation. 1977.

[2] P. Ligrani, R. Moffat. Structure of transitionally rough and fully rough turbulent boundary layers. J. of Fluid Mechanics, 162, 69-98. 1986.

Surface roughness

- The nondimensional roughness height can be computed as follows,

$$K_s^+ = \frac{\rho K_s u^*}{\mu}$$

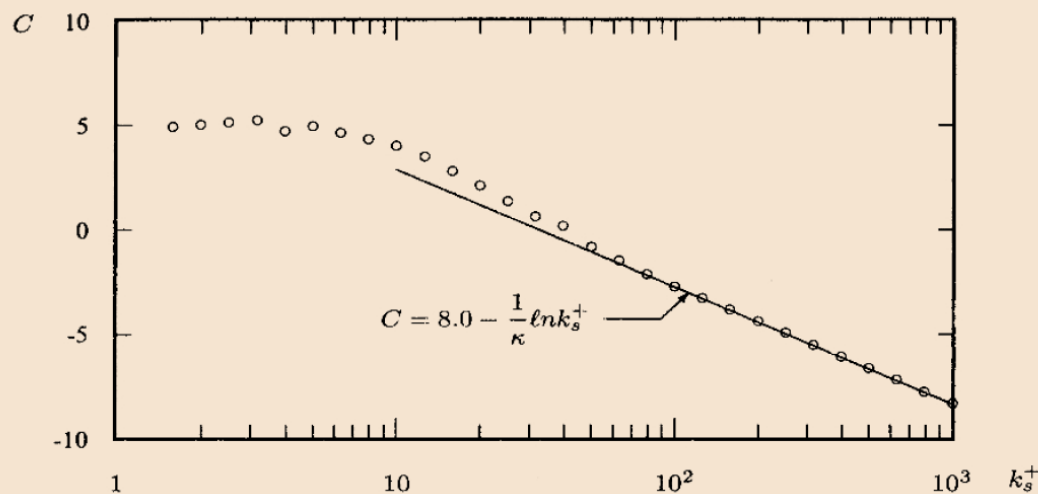


Similar to the approach taken for y^+

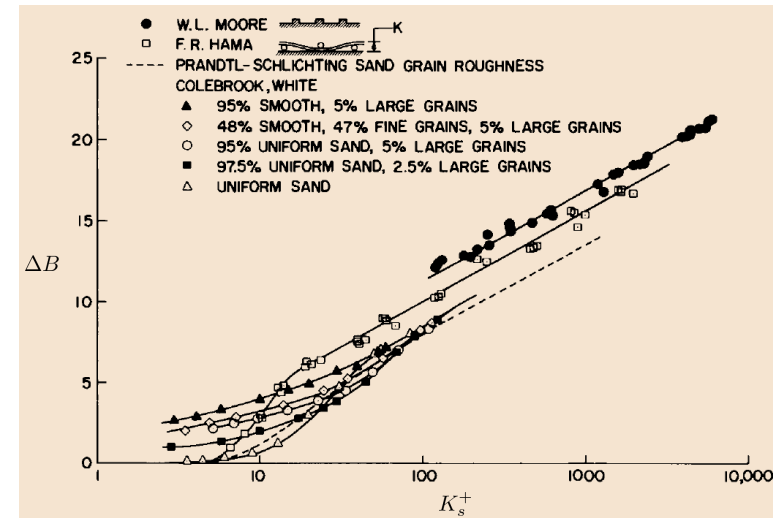
- Where K_s is the typical roughness height (sand grain diameter).
- The roughness constant C_s is often equal to 0.5. This constant represents the shape and distribution of the roughness elements (sand grains).
- It is recommended to fix C_s and adjust K_s^+ .
- Notice that the whole roughness regime is subdivided into the three regimes,
 - The hydraulically smooth condition exists when roughness heights are so small that the roughness is buried in the viscous sublayer.
 - The fully rough flow condition exists when the roughness elements are so large that the sublayer is completely eliminated, and the flow can be considered as independent of molecular viscosity; that is, the velocity shift is proportional to $\ln(K_s^+)$.
 - The transitional region is characterized by reduced sublayer thickness, which is caused by diminishing effectiveness of wall damping. Because molecular viscosity still has some role in the transitional region, the geometry of roughness elements has a relatively large effect on the velocity shift.

Surface roughness

- The subdivision of the roughness regime and the dependence of the constant C (law of the wall) and the roughness correction factor ΔB are supported on experimental data (Nikuradse's data [1]).
- The constant C and the roughness correction factor depend on the roughness parameters K_s^+ and C_s .



Constant in the law of the wall as a function of surface roughness. Based on measurements of Nikuradse [1]. Adapted from [2].



Effect of wall roughness on the roughness correction factor and universal velocity profiles [3].

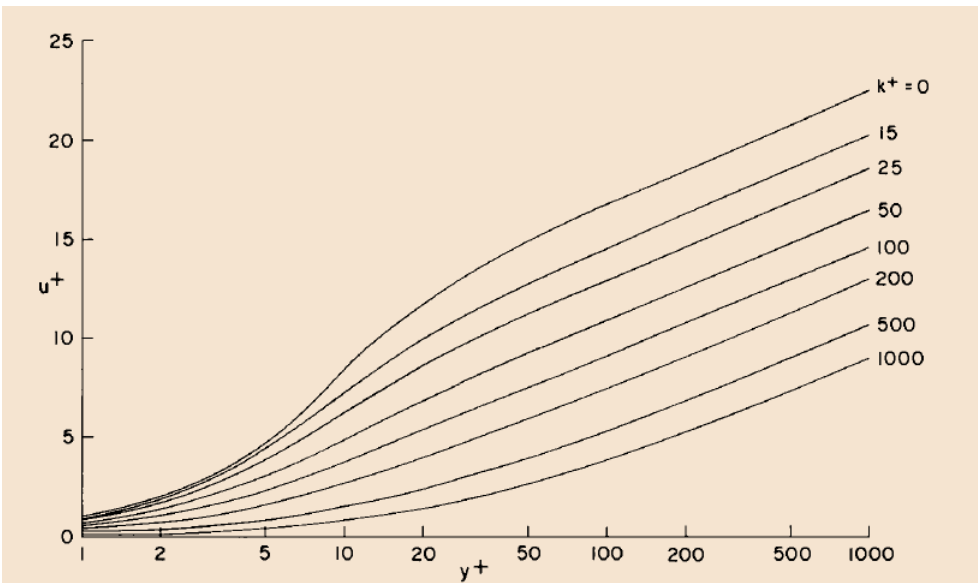
[1] J. Nikuradse. Law of Flow in Rough Pipes. Technical Memorandum 1292, National Advisory Committee for Aeronautics. 1950.

[2] D. Wilcox. Turbulence modeling for CFD. DCW Industries, Inc. 2006.

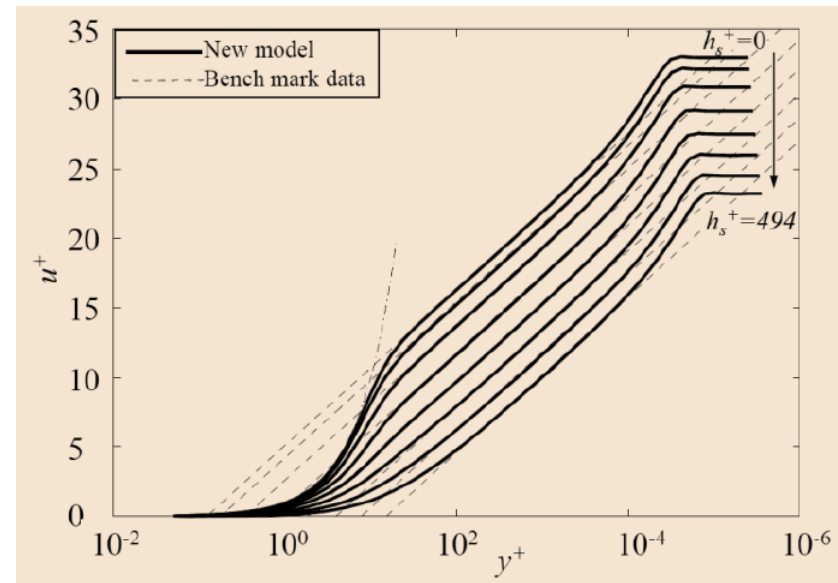
[3] F. Clauser. The turbulent boundary layer. Advan. Appl. Mech. 4, 1. 1956.

Surface roughness

- Plots of mean velocity distribution for uniform roughness at several K_s^+ values.



Plots of mean velocity distribution for uniform roughness at several values of nondimensional roughness height [1].



Plot of roughness mean velocity profiles [2].

[1] T. Cebeci, A. M. O. Smith. Analysis of turbulent boundary layers. Academic Press. 1974.

[2] U. Orij, X. Yang, P. Tucker. Hybrid RANS/ILES for Aero Engine Intake. Proceedings of the ASME Turbo Expo 2014. Paper No: GT2014-26472. 2014.

Surface roughness

- There is no universal roughness function valid for all types of roughness.
- Many methods to take into account the surface roughness are available in the literature, just to name a few,
 - [1] T. Cebeci, P. Bradshaw. Momentum transfer in boundary layers. Hemisphere Publishing Corporation. 1977.
 - [2] P. Ligrani, R. Moffat. Structure of transitionally rough and fully rough turbulent boundary layers. J. of Fluid Mechanics, 162, 69-98. 1986.
 - [3] B. Aupoix, R. Spalart. Extensions of the Spalart-Allmaras turbulence model to account for wall roughness. Int. J. of Heat and Fluid Flow. 24. 2003.
 - [4] D. Wilcox. Turbulence modeling for CFD. DCW Industries, Inc. 2006.
 - [5] U. Orij, X. Yang, P. Tucker. Hybrid RANS/ILES for aero engine intake. Proceedings of the ASME Turbo Expo 2014. Paper No: GT2014-26472. 2014.
 - [6] B. Krishnappan. Laboratory verification of a turbulent flow model. J. of Hydraulic Eng. 110. 1984.
 - [7] J. Yoon, V. Patel. A numerical model of flow in channels with sand-dune beds and ice covers. IIHR Report no. 362. 1993
 - [8] J. Rotta. Turbulent boundary layers in incompressible flows. Progress in Aerospace Science. 1982.
- Finally, a rough wall increases friction, but it happens that special surfaces can increase drag reduction.
- It appears that small riblets that are aligned with the flow direction can achieve a significant drag reduction up to 10%.
- Well designed riblets can shift the nondimensional velocity profile upwards.

Roadmap to Lecture 9

- ~~1. Favre averaging~~
- ~~2. RANS models corrections~~
- ~~3. Wall functions for heat transfer~~
- ~~4. Wall functions – Additional observations~~
- ~~5. Surface roughness~~
- 6. Non-linear eddy viscosity models**

Non-linear eddy viscosity models

- One approach to achieving a more appropriate description of the Reynolds-stress tensor without introducing any additional transport equations (as in the RSM models) is to add extra high order terms to the Boussinesq approximation.

$$\overline{\rho u'_i u'_j} = \frac{2}{3} \rho k \delta_{ij} - 2\mu_t S_{ij} + f(S_{ij}, \Omega_{ij})$$

- Where $f(S_{ij}, \Omega_{ij})$ is a nonlinear function dependent on the mean strain rate tensor S_{ij} and spin tensor (rotation) Ω_{ij} .
- Recall that the mean strain rate tensor and spin tensor are defined as follows,

$$S_{ij} = \frac{1}{2} \left(\frac{\partial u_i}{\partial x_j} + \frac{\partial u_j}{\partial x_i} \right) \quad \Omega_{ij} = \frac{1}{2} \left(\frac{\partial u_i}{\partial x_j} - \frac{\partial u_j}{\partial x_i} \right)$$

- These models are known as nonlinear eddy viscosity models (NLEVM).
- This idea was originally proposed by Lumley [1,2], and many NLEVM has been proposed since then.

[1] J. Lumley. Toward a turbulent constitutive equation. Journal of Fluid Mechanics. 1970.

[2] J. Lumley. Computational modeling of turbulent flows. Advances in Applied Mechanics. 1978.

Non-linear eddy viscosity models

- The NLEVM approach can be seen as a remedy to the deficiencies of the EVM.
- Where the main deficiencies of the EVM are:
 - Inability to properly describe the anisotropic behavior in shear layers. In the EVM the normal stresses are isotropic, $\overline{u'^2} = \overline{v'^2} = \overline{w'^2} = (2/3)k$.
 - Flow in ducts with secondary motions.
 - Overpredicting production of turbulent kinetic energy in stagnation points.
 - Failure to reproduce the asymmetric behavior of the velocity profiles in the presence of streamlined geometries (strong curvature).
 - Underpredicting turbulent viscosity in the presence of system rotation (strong vortices).
- In comparison to the EVM, the NLEVM models are more computationally expensive (as they need to solve more terms and are wall resolving).
- They are also harder to converge.
- However, they do offer improved prediction capabilities for certain complex turbulent flows.
- Despite the many apparent advantages of NLEVM, they are not widely used.
- EVM still are the workhorse of turbulence modeling.

Non-linear eddy viscosity models

- The NLEVM are usually quadratic or cubic.
- Let us briefly discussed the NLEVM by Shih et al [1], which is cubic.
- In this model, the Reynolds stresses are computed as follows,

$$-\overline{\rho u'_i u'_j} = -\frac{2}{3}\rho k \delta_{ij} + \mu_t 2S_{ij}^* + A_3 \frac{\rho k^3}{\epsilon^2} [\bar{S}_{ik} \bar{\Omega}_{kj} - \bar{\Omega}_{ik} \bar{S}_{kj}]$$

$$-2A_5 \frac{\rho k^4}{\epsilon^3} \left[\bar{\Omega}_{ik} \bar{S}_{kj}^2 - \bar{S}_{ik}^2 \bar{\Omega}_{kj} + \bar{\Omega}_{ik} \bar{S}_{km} \bar{\Omega}_{mj} - \frac{1}{3} \bar{\Omega}_{kl} \bar{S}_{lm} \bar{\Omega}_{mk} \delta_{ij} + I_s S_{ij}^* \right]$$

- Where I_s , S_{ij}^* , and S_{ij}^2 are given by the following relationships,

$$I_s = \frac{1}{2} [\bar{S}_{kk} \bar{S}_{mm} - \bar{S}_{kk}^2] \quad S_{ij}^* = \bar{S}_{ij} - \frac{1}{3} \bar{S}_{kk} \delta_{ij} \quad S_{ij}^2 = \bar{S}_{ik} \bar{S}_{kj}$$

Non-linear eddy viscosity models

- This model is particularly suited for swirling flows.
- It as developed to deal with aircraft engine combustors that generally involve turbulent swirling flows in order to enhance fuel-air mixing and flame stabilization.
- The model includes third order terms, so it offers extra accuracy.
- The method also satisfy the constraints of rapid distortion theory (RDT) and realizability.
- All the coefficients appearing in the nonlinear constitutive equation are calibrated using DNS and experimental data.
- The coefficient C_μ is not constant. It depends on the strain rate tensor.
- The value of the turbulent kinetic energy k and the dissipation rate ϵ are obtained from low-RE $k - \epsilon$ turbulence models (wall resolving).
- Also, the value of the turbulent eddy viscosity is computed using the relations from low-RE $k - \epsilon$ turbulence models.